Technical Overview

Shielding Charged Particle Emission from Ion Pumps

New sizes and Agilent StarCell Element

Author

P. Manassero
Agilent Technologies Inc.

Abstract

This technical overview reports the study of the emission of charged particles from ion getter pumps (IGP) and the design and testing of particle shielding. It represents the completion of the study described in the paper "Shielding Charged Particle Emission from Ion Pumps".[1] After tests aimed to understand the degree to which particles are emitted from an IGP, an optimized optical shield was designed and tested for both diode and Agilent StarCell pumping elements. The goal was to maximize the charged particle shielding effect, while minimizing the impact on pumping speed as much as possible.

Introduction

At the heart of an ion getter pump (IGP) is the Penning cell, made up of a cylindrical anode and planar cathode surfaces, which use electric and magnetic fields to trap electrons.[2] These trapped electrons ionize gas molecules that are then accelerated towards a titanium cathode. Due to ion impacts on the cathode, titanium atoms are sputtered onto the inner surfaces of the IGP. This constantly refreshed film of titanium acts as an active getter material and can pump getterable gas molecules by chemisorption. Typically, IGPs have an array of multiple Penning cells. The ion current in each cell (and therefore, the total current of the IGP) is directly proportional to the gas pressure; the intensity of the discharge is defined as the current divided by the pressure (IP). Gaps exist between the cylindrical anode array and the planar cathodes on each end. Particles can escape the Penning cells through these gaps and strike surfaces within the IGP, or pass into the vacuum facility to which the IGP is connected. The image in Figure 1 shows plasma formation in a Penning cell array with the anode-cathode gaps indicated. From these gaps, particles can escape, such as photons, neutral molecules (e.g., sputtered titanium) and charged particles.

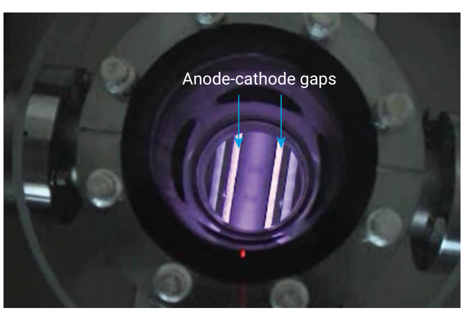

Figure 1. View through a window placed on top of an ion pump operating at a pressure of ~1×10^{-4} mbar.

Ion getter pumps are typically used in the range from 1×10^{-7} mbar down to 1×10^{-11} mbar or lower. Two typical applications, among many others, are high-energy physics (HEP) particle accelerators and scanning electron microscopes (SEM). In these applications, the required vacuum level is in the range of at least 1×10^{-8} mbar and down to 1×10^{-10} mbar. These vacuum levels are required to reduce beam losses and improve image resolution, due to the fact that the lower the pressure, the lower the probability of collisional scattering of beam particles (protons, ions, or electrons) by the residual gas. Such interactions affect the beam quality (focus, energy, etc.) and therefore reduce the performance of the system. While they provide the required vacuum, IGPs can emit particles that interfere with device operation. To prevent negative effects, such as titanium sputtering onto sensitive elements of the system, it is common practice to introduce so-called "optical shielding" that interrupts the line of sight between the IGP and the system. These shields reduce the gas conductance between the system and the Penning cells, and can therefore reduce the effective pumping speed. Consequently, their shape and relative position with respect to the flange must be carefully evaluated.

Shield designs

Diode pumps

Agilent Vacuum (previously Varian Inc.) has been selling ion pumps equipped with shields for many years.[3,4] The shield configurations described in this paper represent the latest proposed versions, whose position and design have been improved recently with respect to previous implementations.

In this section, the shielding designed for IGPs equipped with a diode pumping element is described. It comprises a horizontal flat surface and a vertical baffle (Figure 2A) that work in conjunction to prevent particles emitted by the ion pump from escaping into the vacuum chamber, as well as blocking the emission of secondary particles (e.g., electrons) from the internal surfaces of the pump. The shield is placed under the flange (Figures 2B and 2C) and is connected to the anode, so that it is polarized at the same voltage at which the pump is operated (typically 3, 5, or 7 kV).

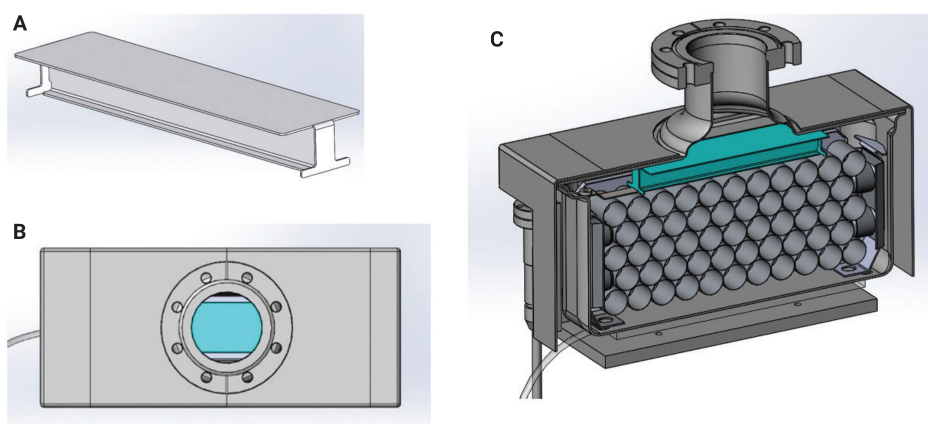

Figure 2. (A) Sketch of the shield designed for the Agilent D-VIP40$_{shield}$, D-VIP55$_{shield}$, and D-VIP75$_{shield}$; (B) Top view of the Agilent D-VIP40$_{shield}$, showing the shield's position inside the pump; (C) Lateral view of the Agilent D-VIP40$_{shield}$: the vertical baffle is welded to the anode of the pumping element.

Agilent Vaclon Plus (VIP40, VIP55 and VIP75) ion pumps differ only in the inlet flange dimensions and can be equipped with a diode or Agilent StarCell element. In this paper, the diode pumps are identified by the letter "D" in their name and the StarCell pumps with "SC".

The shield described above and shown in Figure 2 is used for the D-VIP40$_{shield}$, D-VIP55$_{shield}$ and D-VIP75$_{shield}$ pumps.

StarCell pumps

The StarCell element is the improved version of the triode element. Distinct from the diode element, in which the cathodes are grounded and the anode is fed with positive voltage, the StarCell element's anode is grounded, and the cathodes are negatively biased and separated from the pump body. In this configuration, the anode and the surfaces of the pump body become the positive poles of the triode structure, so that titanium atoms can be sputtered from the cathodes, not only on the anode but also on the pump walls, which become active components in pumping the gas.

Figure 3. The Agilent StarCell element: The shape of the cathode, which is made of stars with small formed wings, is optimized to pump noble gases and to ensure a longer lifetime.[4]

Considering the characteristics of the StarCell element, the same shielding conceived for diode pumps cannot be used for StarCell pumps. Therefore, a new dedicated shield has been designed for a medium-sized pump equipped with a StarCell element. As the diode pump's shielding, it comprises a horizontal top plate and a vertical baffle. It works by combining optical and electrical effects to block particles: the position between the inlet flange and the pumping element ensures an optical shielding effect (Figure 4A), while to achieve electrical shielding, the top plate is connected to the cathode so that it is polarized at the same voltage at which the pump is operated.

It is worth pointing out that diode and StarCell pumps are fed with positive and negative voltages respectively, so that the two shielding configurations are fed with opposite polarities. The assumption, confirmed by test results, is that both positive and negative voltages applied to the shield can provide a blocking effect. In fact, both attraction and repulsion effects due to the shield's polarization can deflect the trajectory of charged particles when they are escaping the pump through the inlet flange, causing some of them (depending on their energy) to remain in the pump's internal volume. Additionally, in IGPs, both ions and electrons are present, so it is not possible to select a single type of electrical interaction (attraction/repulsion) of particles with the shield, irrespective of polarization.

The vertical baffle, which blocks the emission of secondary particles from the internal surfaces of the pump, is made of two semibaffles: one connected to the shield's top plate, and the other connected to the pumping element (Figure 4B). In this way, the line of sight between the top plate of the shield and the pumping element is fully interrupted, while electrical insulation between the cathode and the anode is preserved.

To minimize the impact on the pumping speed from the SC-VIP55$_{shield}$ and SC-VIP75$_{shield}$, the shield introduced in these pumps presents an elliptical hole (Figure 4C). Thus, the gas molecules can easily enter the anode-cathode-gap area, where they can be ionized after interaction with free electrons, to be pumped. The negative impact of the hole on the shielding efficiency can affect the optical shielding effect, but the impact on the electrical shielding effect is negligible and is mitigated by maximized extension of the top plate surface.

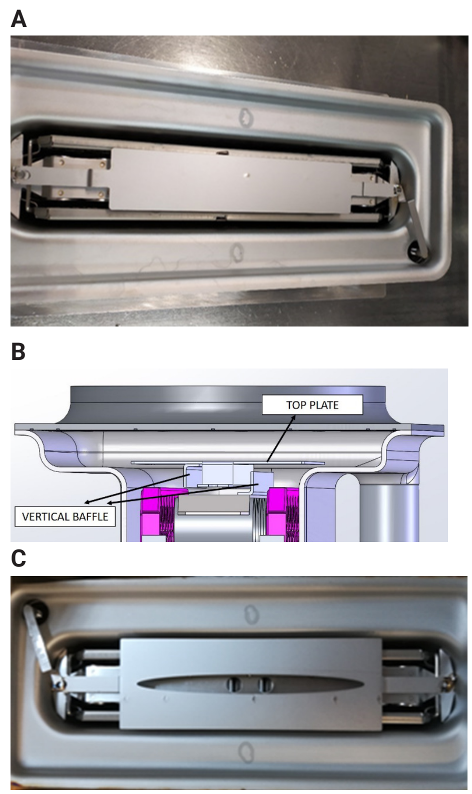

Figure 4. (A) View of the shield for the Agilent SC-VIP40$_{shield}$ (as in Figure 2C); (B) Front view of the shield for the Agilent SC-VIP55$_{shield}$ and Agilent SC-VIP75$_{shield}$ (the vertical baffle has the same design for both shielding configurations); (C) Top view of the shield for the Agilent SC-VIP55$_{shield}$ and Agilent SC-VIP75$_{shield}$.

Experimental

Experimental measurements were carried out to study the physical phenomenon of particle emission and to analyze the efficiency of shielding in blocking these particles. To achieve these goals, a comparison was made between same-size IGPs that differed only in the presence or absence of the shield. Specifically, standard Agilent ion pumps VIP40, VIP55, and VIP75 (Figures 5A to 5C) equipped with diode and StarCell pumping elements, and same-size special pumps with the shield were tested. All pumps were tested using the experimental setup shown in Figure 6.

A

B

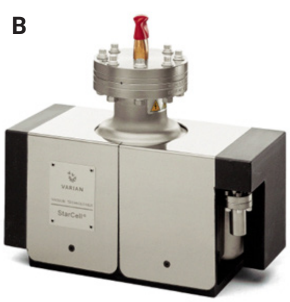

C

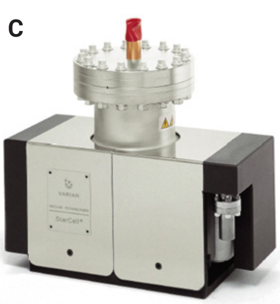

Figure 5. (A) Agilent Vaclon Plus 40 Pump. (B) Agilent Vaclon Plus 55 Pump. (C) Agilent Vaclon Plus 75 Pump.

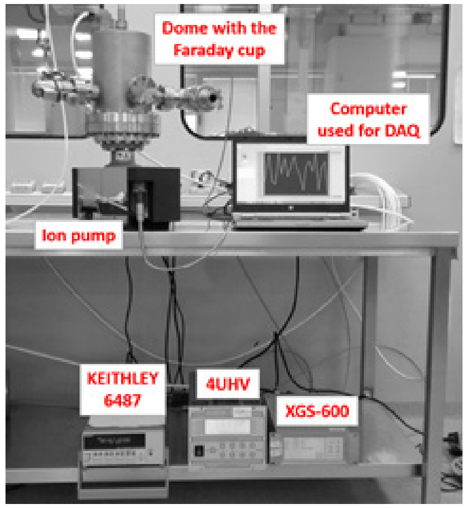

Figure 6. Experimental setup used for measurements.

A conical copper Faraday cup was positioned in a vacuum chamber above the flange of the ion pump (as shown in Figure 7) to measure the current generated by the charged particles which escaped from the pump.

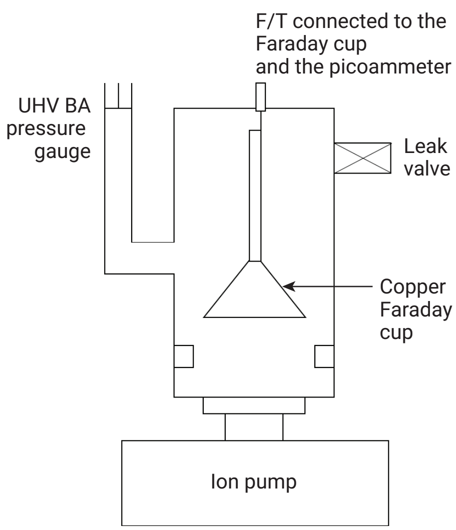

Figure 7. Sketch of experimental setup showing the Faraday cup placed inside the dome above the ion pump under test.

A Faraday cup (Figure 8) is a conductive metal electrode designed to measure the current induced by particles incident on the cup. (This kind of detector is named after Michael Faraday, who first theorized ions around 1830.) This current can be measured by an ammeter, and is used to estimate the flux of particles hitting the cup. A bias voltage applied either to the cup itself or a repelling grid preceding the cup (or magnetic field) are often used to control the polarity of particles incident on the cup, or to prevent secondary electron emission from distorting the reading. The design can be significantly more complicated when it is necessary to make measurements of very short pulses or very high energy beams that may not be fully stopped by the thickness of the detector. This device is a nearly universal detector due to its ability to detect particles largely independent of the energy, mass, or species of the analyte. When using a Faraday cup to count the number of charged particles collected per unit time, there can be several sources of error, including: (1) the emission of low-energy secondary electrons from the surface struck by any incident particle with sufficient energy (ions, electrons, photons, high-energy neutral atoms/molecules) and (2) field emission of electrons directly from the Faraday cup itself. It is fundamentally impossible to distinguish between one or more incident ions and secondary

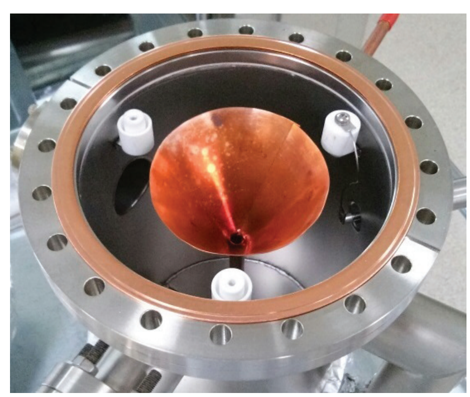

Figure 8. Copper Faraday cup used for the tests.

electrons emitted from the cup due to high-energy particle impacts, or field-emitted electrons. Even if the Faraday cup does not clearly allow us to distinguish between particles due to these complications, from an end user's perspective, the particular species of particle(s) is likely not important; only the fact that charged particles or energetic particles in general are being emitted is relevant. Despite these limitations, it was assumed that the Faraday cup was sufficient to estimate the relative rate of particle emission for different pumps and configurations, to assess the efficacy of shielding.

The cup was polarized with a voltage in the range of –500 to +500 V to measure the current-versus-voltage (I/V) curve. As stated above, the positive (or negative) bias of the cup does not strictly mean selective detection of exclusively negatively (or positively) charged particles. For example, when the Faraday cup is biased at a negative voltage, a positive current is measured, (mostly due to the ions emitted by the pump) but increased by the escape of secondary electrons from the cup itself.

A picoammeter/voltage-source was used for reading the current generated by the particle emission from the IGP, and for polarizing the Faraday cup. The pressure in the vacuum chamber was measured with an Agilent UHV-24 ionization gauge, with the possibility of increasing it by introducing dry nitrogen into the dome through a variable leak valve. After verifying that the current collected by the Faraday cup increased linearly with the pressure, the amount of nitrogen in the vacuum chamber was held constant in the mid 10^{-7} mbar range for all measurements.

Results and discussion

Particle emission test: diode pumps

All pumps were tested by measuring the current collected by the Faraday cup as a function of the bias applied to the cup in the range of –500 to +500 V. As discussed previously, the current collected by the Faraday cup is proportional to the amount of the detected particles, but it does not allow determination of the absolute number of particles or their energy, due to secondary electrons. Figure 9 shows the current (I_{cup}) as a function of the voltage (V_{cup}) for the D-VIP40 and D-VIP40$_{shield}$.

The shape of the curve is similar for both pumps, but the magnitude of the current detected for the D-VIP40 is approximately 30 nA, while that detected for the D-VIP40$_{shield}$ is only ~10 pA (a factor of 3,000 lower). This significant difference indicates that the shield with which the D-VIP40$_{shield}$ is equipped works very efficiently in reducing the emission of particles from the ion pump. Agilent VIP40, VIP55, and VIP75 pumps differ only in inlet flange dimensions, while the pumping element and the pump body remain the same.

- VIP40 inlet flange diameter: 2 ¾ in.
- VIP55 inlet flange diameter: 4.5 in.
- VIP75 inlet flange diameter: 6 in.

Figures 10 and 11 show the results on the D-VIP55$_{shield}$ and D-VIP75$_{shield}$ diode pumps, compared with equivalent standard versions of the pump (without shielding). As expected, the overall current increases with the inlet flange dimensions.

Comparing the shielded pumps with the standard pumps, findings show that the shield causes a decrease of the measured current by two orders of magnitude. Thus, the shielding efficiency is lower than observed on the D-VIP40$_{shield}$, but still leads to a significant improvement.

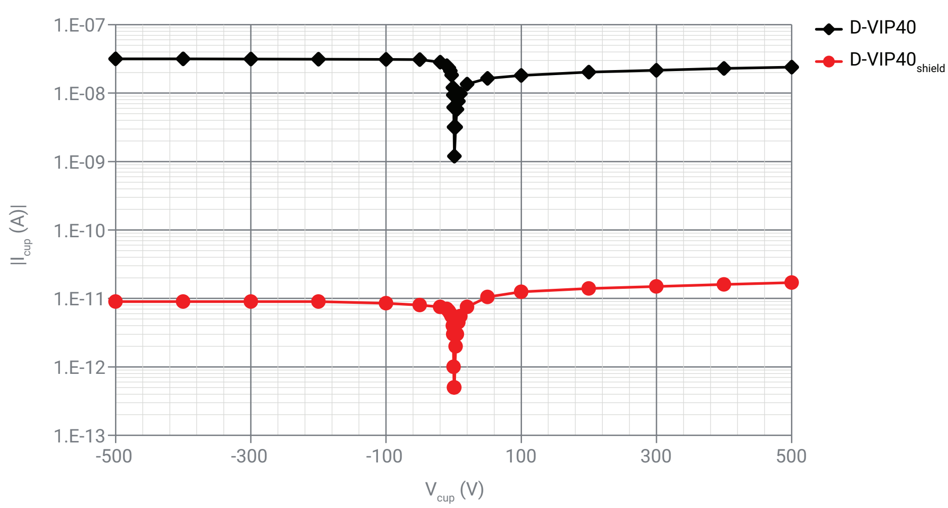

Figure 9. Overlaid curves of the absolute value of collected current for the Agilent D-VIP40$_{shield}$ and Agilent D-VIP40 (logarithmic scale).

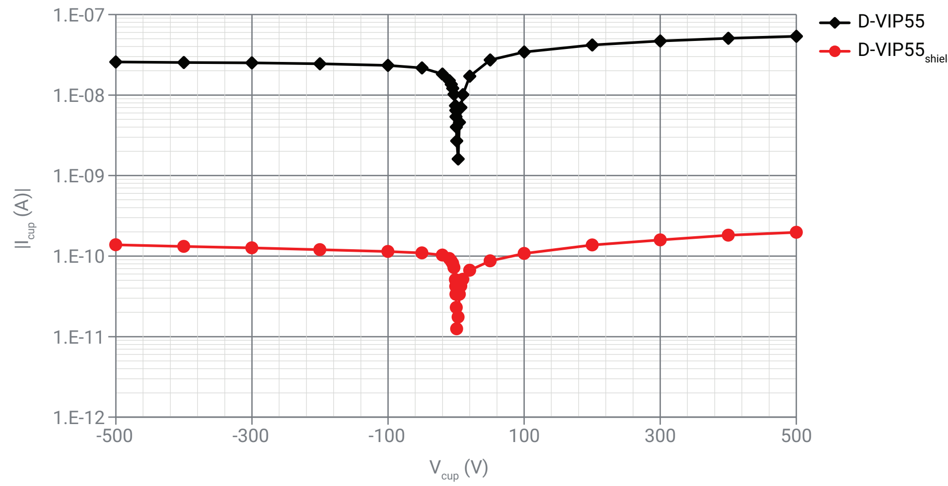

Figure 10. Overlaid curves of the absolute value of collected current for the Agilent D-VIP55$_{shield}$ and Agilent D-VIP55 (logarithmic scale).

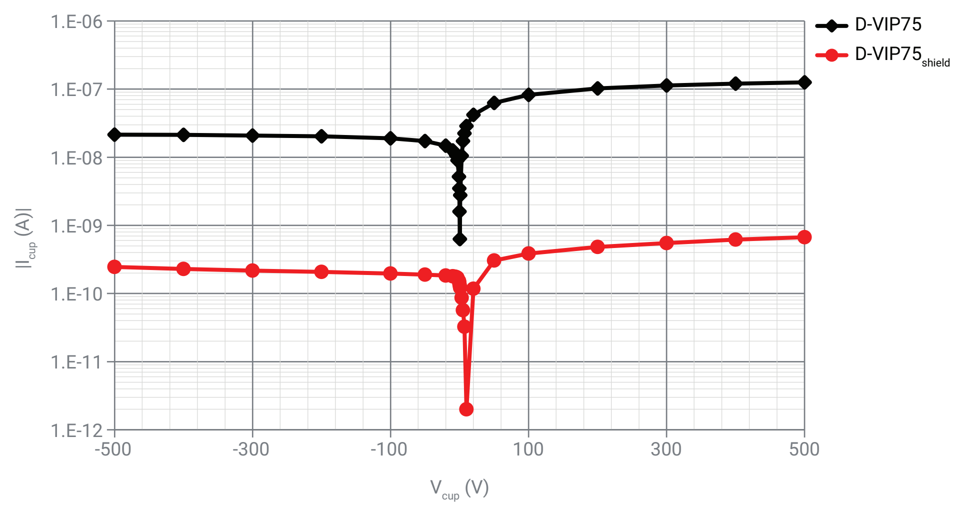

Figure 11. Overlaid curves of the absolute value of collected current for the Agilent D-VIP75$_{shield}$ and Agilent D-VIP75 (logarithmic scale).

Particle emission test: StarCell pumps

In this section, the results of the current emission measurement on the pumps equipped with the StarCell pumping element are reported. As shown in Figures 12 to 14, the trend of the current as a function of the voltage applied to the Faraday cup is similar to that observed on diode pumps, but the current values are quite different. Most of the current values measured on SC-VIP40, SC-VIP55 and SC-VIP75 standard pumps are in the range of 10^{-8} A, the same as the current measured on diode standard pumps. Thus, the particle emission effect seems to be independent of (or very weakly dependent on) the pumping element type. For every pump size, the overall current level measured on shielded pumps is one order of magnitude lower than the current measured on the corresponding standard pumps. Even if the shielding efficiency is lower than that obtained for diode pumps, the shield still leads to an appreciable current decrease. At this stage of the study, the reason why the StarCell shielding has a lower blocking efficiency than that provided by the diode shielding is not clear. One hypothesis is that the triode structure (and its own pumping mechanism) of the StarCell element brings a greater number of charged particles to move around the whole pump's internal volume, while in diode pumps, almost all particles are confined inside the pumping element in the anode-cathode-gap area. This would result in an intrinsic limit for particle emission shielding based on optical and electrical effects in StarCell pumps. However, more tests with a more sensitive detector are needed to verify this or other hypotheses (the limits of the Faraday cup detector are discussed in the Experimental section). The graphs in Figure 16, concerning SC-VIP40 and SC-VIP40$_{shield}$ curves show that the ratio between standard and shielded pump current is almost constant through the entire Faraday cup voltage range—but the same cannot be said when observing

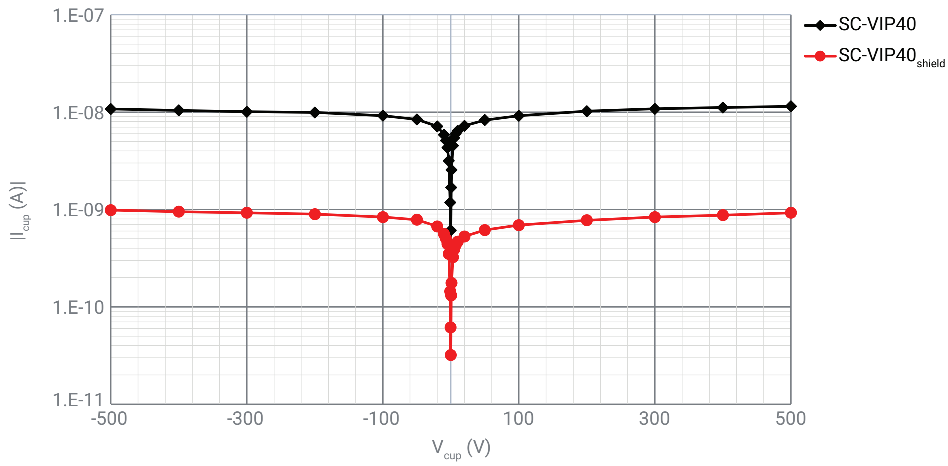

Figure 12. Overlaid curves of the absolute value of collected current for the Agilent SC-VIP40$_{shield}$ and Agilent SC-VIP40 (logarithmic scale).

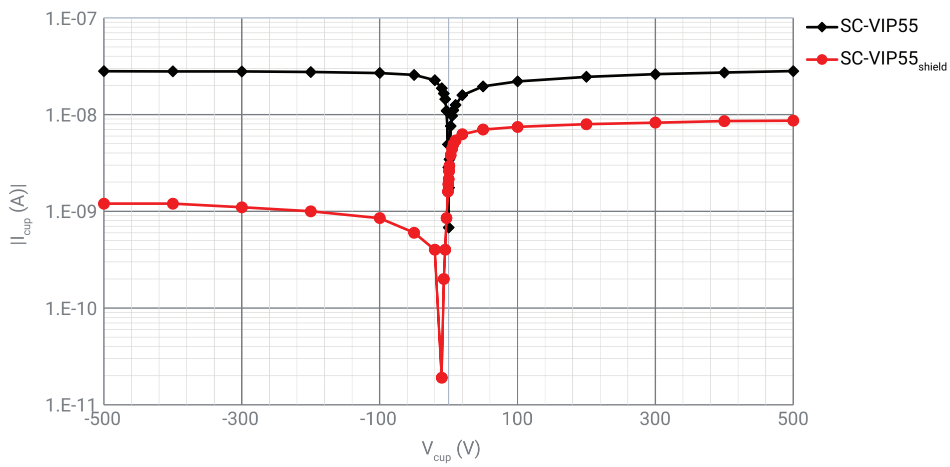

Figure 13. Overlaid curves of the absolute value of collected current for the Agilent SC-VIP55$_{shield}$ and Agilent SC-VIP55 (logarithmic scale).

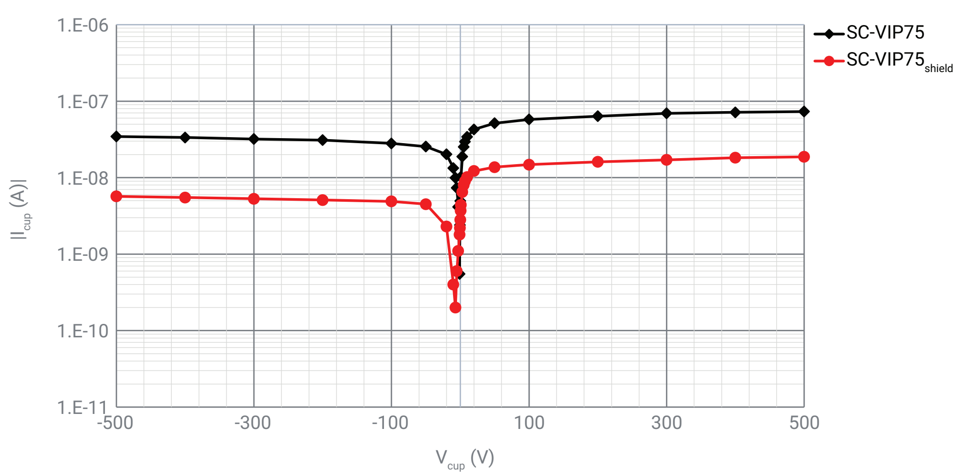

Figure 14. Overlaid curves of the absolute value of collected current for the Agilent SC-VIP75$_{shield}$and Agilent SC-VIP75 (logarithmic scale).

SC-VIP55 and SC-VIP55$_{shield}$ curves (Figure 15), since the SC-VIP55$_{shield}$ curve presents an evident asymmetry between its left (negative voltages) and right (positive voltages) halves. The reason for the asymmetrical trend cannot be easily guessed; it may be related to the particular shape of the SC-VIP55$_{shield}$ shielding, which can cause a different shielding efficiency for ions (heavier and positively charged) and electrons (lighter and negatively charged) because of the presence of the central hole, but this or other hypotheses would require further tests to be verified.

Pumping speed test: diode pumps

As a consequence of the implementation of shields inside the IGPs with the goal of reducing particle emission, the gas conductance is reduced and the effective pumping speed of the pump is also unavoidably lowered. To determine the effect of the shield on the D-VIP40$_{shield}$ pump, a Fischer-Mommsen dome[4] was used to measure pumping. Each curve represents the average of at least three measurements carried out on the same pump. The pumping speed curve of the D-VIP40 is also shown for reference.

Please note that the measured curves in Figure 15 (and in following graphs) start in the low 10^{-9} mbar range (since for all pumps, the achieved base pressure after a mild bakeout (approximately 12 hours at 180 °C) and after saturation with nitrogen, was in the mid 10^{-10} mbar range).

As expected, the D-VIP40 exhibits the best pumping speed performance,

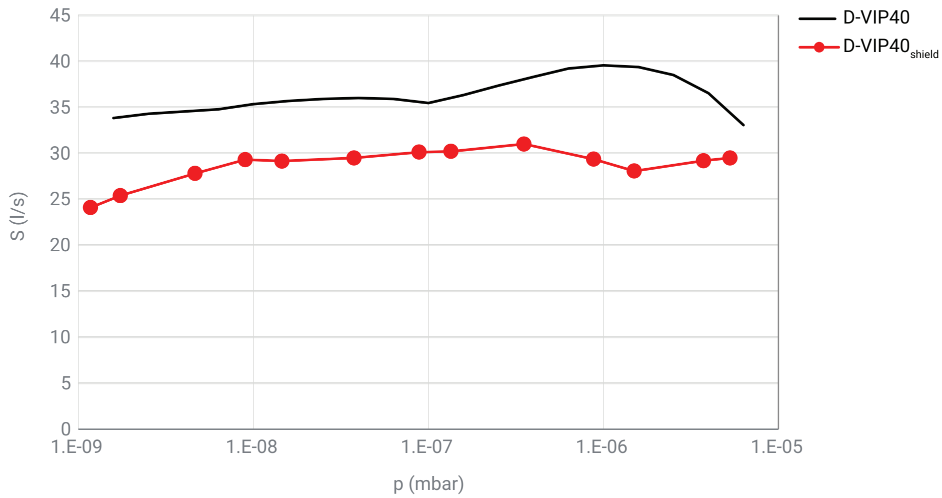

Figure 15. Saturated pumping speed curves (nitrogen) for the Agilent D-VIP40 and Agilent D-VIP40$_{shield}$.

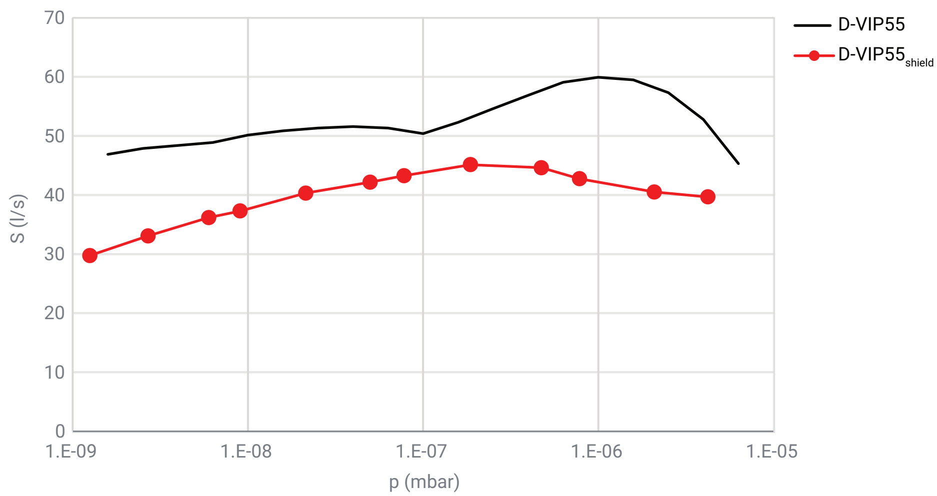

Figure 16. Saturated pumping speed curves (nitrogen) for D-VIP55 and D-VIP55$_{shield}$.

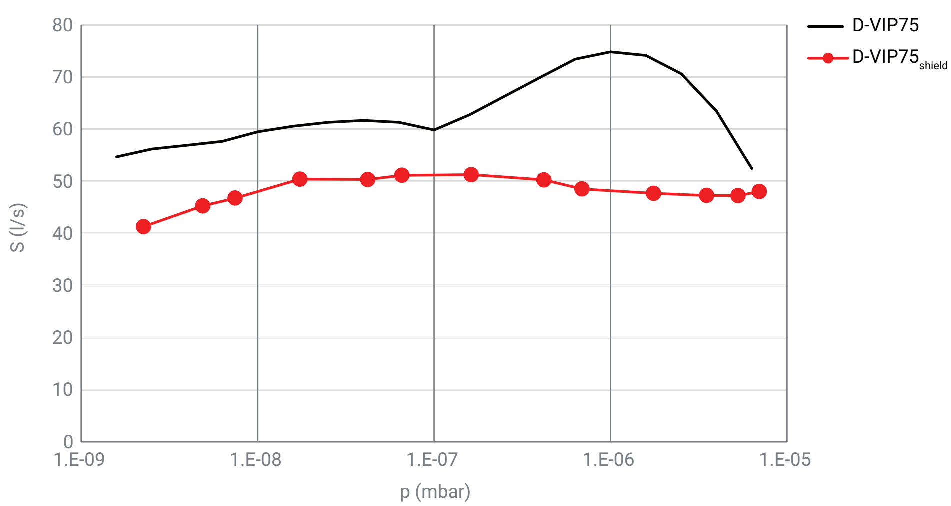

Figure 17. Saturated pumping speed curves (nitrogen) for D-VIP75 and D-VIP75$_{shield}$.

since no shields are mounted inside. Considering the maximum value of each curve (which corresponds to a pressure of approximately 4×10^{-7} mbar), 31 L/s was measured for the D-VIP40$_{shield}$, 23% lower than for the D-VIP40. In Figure 16, the pumping speed curves of D-VIP55 and D-VIP55$_{shield}$ are reported, while Figure 17 shows the pumping speed curves of D-VIP75 and D-VIP75$_{shield}$.

For both the D-VIP55$_{shield}$ and D-VIP75$_{shield}$, the maximum pumping speed value corresponds to a pressure of about 2×10^{-7} mbar. The maximum value of the D-VIP55$_{shield}$ is 45 L/s, which corresponds to a reduction of 18% with respect to a standard D-VIP55. The maximum value of D-VIP75$_{shield}$ is 51 L/s, resulting in 32% loss of performance in terms of pumping speed when compared to the D-VIP75.

A summary of the nominal pumping speed (i.e. the maximum value of each curve) obtained on all diode pumps is shown in Table 1.

Pumping speed test: StarCell pumps

As discussed, the presence of the shield leads to reduced gas conductance, and consequently, to a significant pumping speed loss. For diode pumps, the measurements were executed using a Fischer-Mommsen dome[5] and each curve represents the average of at least three measurements carried out on the same pump. As StarCell pumps are commonly used when noble gas capacity is required, the results for argon are reported, as well as nitrogen pumping speed (Figures 18 to 20). The summary of the nominal pumping speed obtained on all StarCell pumps (reported in Table 2) requires consideration for two reasons: First, the influence on the nitrogen pumping speed of the shield is almost the same for each size, just above 20%. Additionally, when considering the results obtained with argon, the influence of the specific

Table 1. Summary of nominal pumping speed values of diode pumps and the percentage loss due to the presence of the shield.

Pump	Nominal Pumping Speed for Nitrogen (L/s)	Percent Reduction wrt. Standard
Agilent D-VIP40	40	–
Agilent D-VIP40$_{shield}$	31	23%
Agilent D-VIP55	55	–
Agilent D-VIP55$_{shield}$	45	18%
Agilent D-VIP75	75	–
Agilent D-VIP75$_{shield}$	51	32%

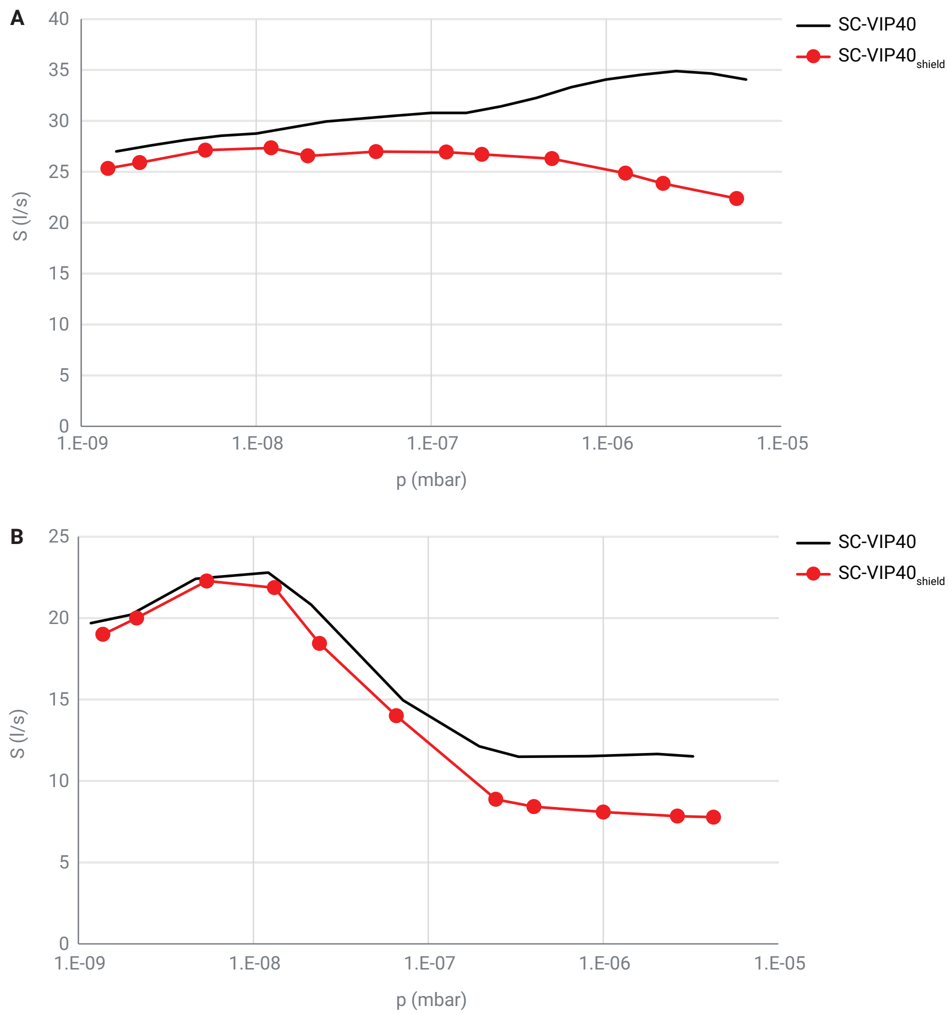

Figure 18. Saturated pumping speed curves for the Agilent SC-VIP40 and Agilent SC-VIP40$_{shield}$ for nitrogen (A) and argon (B).

shield design on the pumping speed is evident: on one hand, the shield introduced in the SC-VIP40$_{shield}$ has a very small impact on pump performance; on the other hand, the shield of the SC-VIP55$_{shield}$ and SC-VIP75$_{shield}$ causes a pumping speed loss of 30 to 35% (considering the nominal values), which is probably due to the extended dimensions of shield's the top plate (refer to the section on StarCell pumps for more information). Nevertheless, the two shielding configurations represent the best state-of-the-art solution for balancing the need for blocking particles from escaping the pump, and the need to preserve a good pumping speed level for StarCell ion pumps.

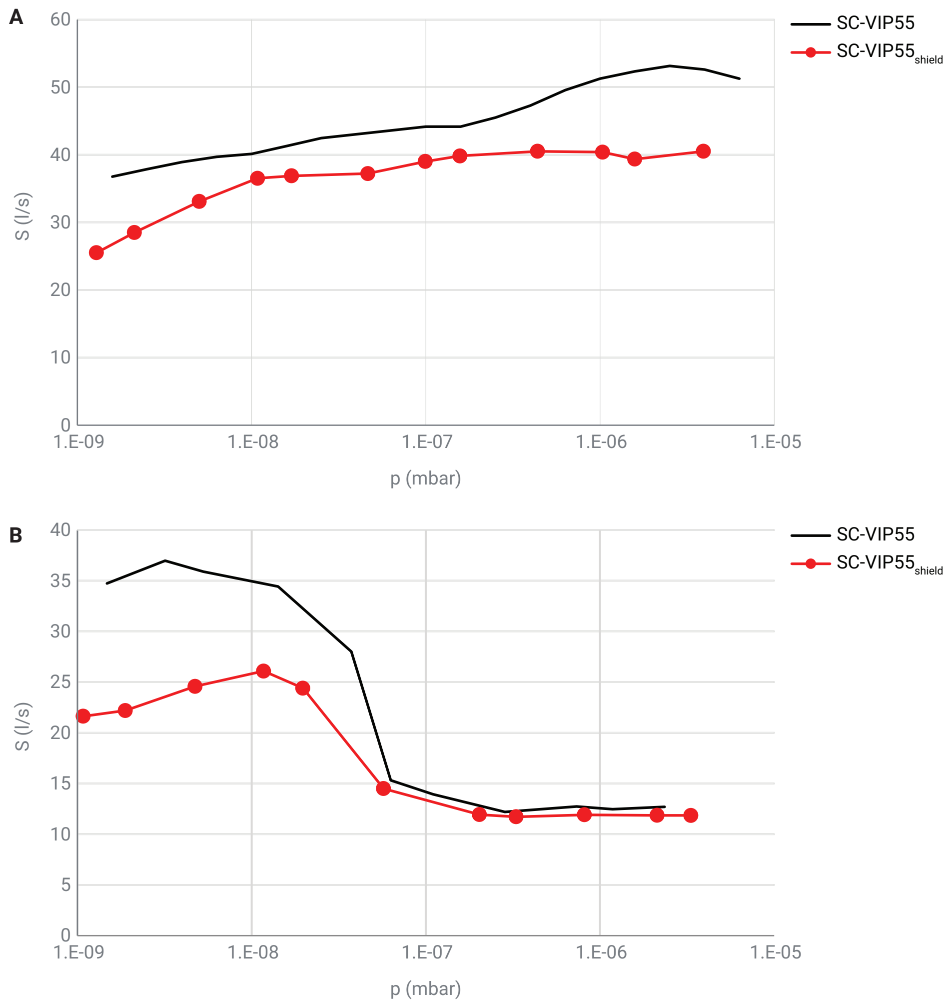

Figure 19. Saturated pumping speed curves for the Agilent SC-VIP55 and Agilent SC-VIP55$_{shield}$ for nitrogen (A) and argon (B).

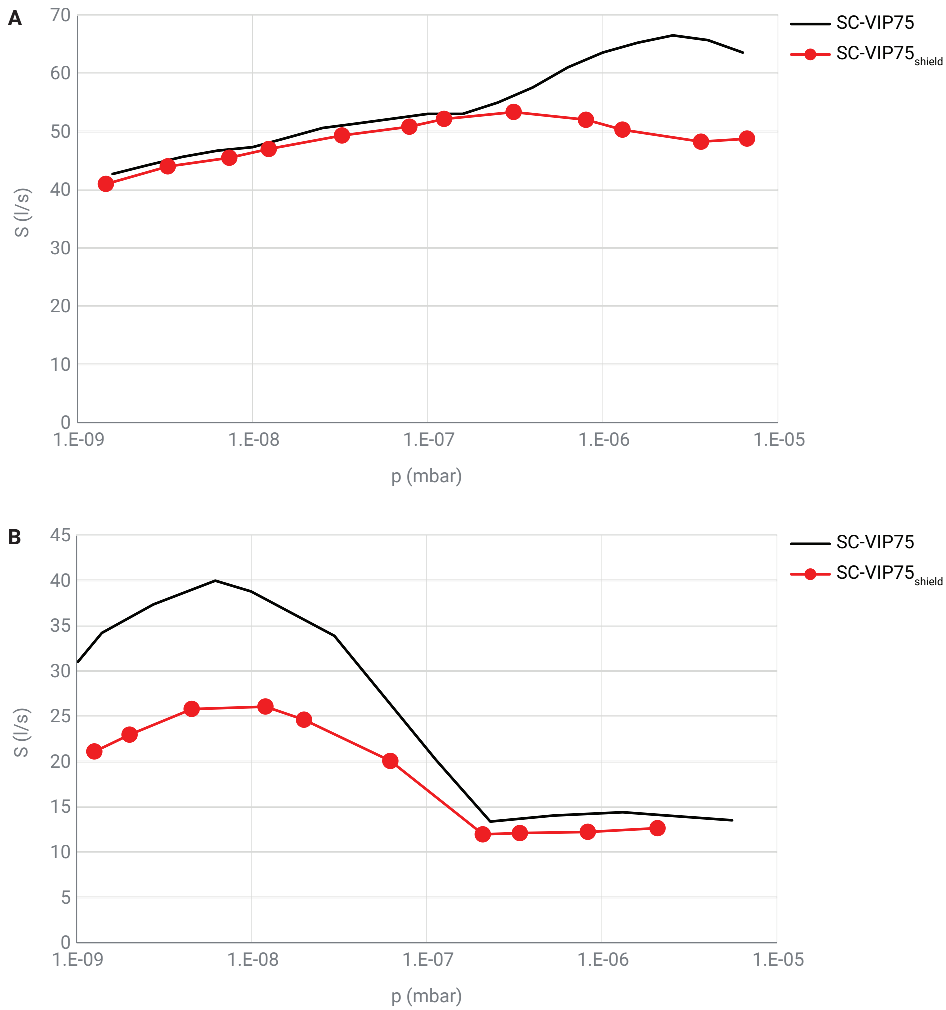

Figure 20. Saturated pumping speed curves for the Agilent SC-VIP75 and Agilent SC-VIP75$_{shield}$ for nitrogen (A) and argon (B).

Table 2. Summary of nominal pumping speed values of Agilent StarCell pumps for nitrogen and argon and the respective percentage loss due to the presence of the shield.

Pump	Nominal Pumping Speed for Nitrogen (L/s)	Percent Reduction wrt. Standard	Nominal Pumping Speed for Argon (L/s)	Percent Reduction wrt. Standard
Agilent SC-VIP40	35	–	23	–
Agilent SC-VIP40$_{shield}$	27	23%	22	4%
Agilent SC-VIP55	53	–	37	–
Agilent SC-VIP55$_{shield}$	41	23%	26	30%
Agilent SC-VIP75	67	–	40	-
Agilent SC-VIP75$_{shield}$	53	21%	26	35%

Conclusion

The experimental tests carried out on the Agilent D-VIP40 and Agilent D-VIP40$_{shield}$ ion pumps have demonstrated that the new shield design in the Agilent ion pump leads to a decrease in the amount of emitted charged particles by a factor of ~1,000, observed as a reduction of the measured current collected by a Faraday cup. Furthermore, the presence of the shield causes a pumping speed loss of 23% with respect to the standard D-VIP40.

The same shield used on the D-VIP40shield is available for the AgilentVIP55 and VIP75 diode pumps (here referred to as the D-VIP55$_{shield}$ and D-VIP75$_{shield}$). On these pumps, the shield induces a reduction of the emission current by two orders of magnitude, while the nominal pumping speed is lowered by 18 and 32%, respectively.

Concerning Agilent StarCell pumps, a new dedicated shield has been introduced, capable of adapting to the StarCell element's characteristics. More specifically, two shields have been designed: one for the Agilent SC-VIP40$_{shield}$, and one for the Agilent SC-VIP55$_{shield}$ and SC-VIP75$_{shield}$s. The working principle of the StarCell element ensures high capacity for noble gases, but represents an intrinsic limit for the shielding efficiency. The SC-VIP40$_{shield}$, SC-VIP55$_{shield}$ and SC-VIP75$_{shield}$s are the best state-of-the-art configurations to balance shielding efficiency and pumping speed: the current emission is lowered by one order of magnitude with respect to equivalent standard pumps (without any shielding) and the nominal pumping speed is lowered by 21 to 23% for nitrogen. Considering argon pumping speed, the shield's effect on the SC-VIP40$_{shield}$ is negligible, while the SC-VIP55$_{shield}$to SC-VIP75$_{shield}$ performance is affected by 30 to 35%.

As a final consideration, it is worth mentioning that the analysis reported in this paper does not address the type of particles being emitted by the ion pumps. The Faraday cup is in fact sensitive to any particles that can induce current, which includes not only ions and electrons, but also neutral particles (photons and neutral atoms/molecules) that can induce secondary electron emission. A more detailed investigation is needed to identify particle species by conducting further experiments with a modified setup.

References

1. Paolini, C. *et al.* Shielding Charged Particle Emission from Ion Pumps. *Agilent Technologies technical overview*, publication number 5991-9269EN, **2018**.
2. Welch, K. M. Capture Pumping Technology, Pergamon Press (1991).
3. Vacuum Solutions for Electron Microscopy Applications, *Varian, Inc. Brochure* July **2005**, 1–12.
4. Paolini, C.; Maccarrone, C. DE Patent No. 10 2016 101 449 A1 (17 March **2016**).
5. Maccarrone, C.; Manassero, P.; Paolini C.; Ion Getter Pumps. Proceedings of the 2017 CERN-Accelerator-School Course on Vacuum for Particle Accelerators, Glumslov (Sweden).
6. DIN28429.

**www.agilent.com/chem/
medium-ion-pumps**

DE26098198

Printed in the USA, July 26, 2021
5991-9269EN

Agilent
Trusted Answers